would occur in dichloroacetic acid in the transition state. An increase in electrostriction due to charge development causes a fairly large volume decrease. The electrostriction around dichloroacetate was estimated as -8 cm^3 mol^{-1} in DMF and -10 cm^3 mol^{-1} in MeCN, according to the modified Drude-Nernst expression $0.5N(2e)^2(r + r')^{-1}\epsilon^{-2}(\partial\epsilon/\partial P)_T$ with the values of $r' = 68$ pm[25] and $(\partial\epsilon/\partial P)_T = 3.406 \times 10^{-2}$ MPa^{-1} [26] for DMF and $r' = 81$ pm[25] and $(\partial\epsilon/\partial P)_T = 4.102 \times 10^{-2}$ MPa^{-1} [27] for MeCN. Since a proton should be solvated more extensively in a basic solvent like DMF than in a less basic solvent such as MeCN, the electrostriction by a proton should be more negative in MeCN than in DMF. Then, if the partial charge separation of DCA is assumed to occur in the activated state for the acid-assisted path, the volume of activation for the dissociation of sodium cryptate may thus be interpreted qualitatively.

Activation parameters for the k_{d1} path in Me_2SO and DMF are quite similar to each other. This suggests that the dissociations proceed in much the same manner in both solvents.

The dissociation of sodium cryptate proceeds through two parallel paths: the solvent path (i.e., acid-independent path) and the acid-assisted path. In Me_2SO, which is the most basic solvent, the solvent path prevails, while in MeCN, which is the least basic solvent, the solvent path is not appreciable and only the acid-assisted path is observed. In DMF, which is moderately basic, both the solvent path and the acid-assisted path are operative in the dissociation of the sodium cryptate.

Acknowledgment. We gratefully thank Dr. H. Yokoyama (Yokohama City University) for experimental information on conductometric measurement. This work was financially supported by a Grant-in-Aid for Scientific Research (Grant No. 62470041), a Grant-in-Aid for Special Project Research (Grant No. 62124039), and a Grant-in-Aid for Developmental Scientific Research (Grant No. 62840019) from the Japanese Ministry of Education, Science and Culture.

Registry No. $NaCry^+$, 32611-86-2.

Supplementary Material Available: Observed rate constants at various concentrations (Tables SI and SII), temperatures (Tables SIII-SV and Figures S1 and S2), and pressures (Tables SVI-SVIII) (10 pages). Ordering information is given on any current masthead page.

(25) Tanaka, N.; Ogata, T. *Inorg. Nucl. Chem. Lett.* **1974**, *10*, 511.
(26) Moriyoshi, T., unpublished results.
(27) Srinivasan, K. R.; Kay, R. L. *J. Solution Chem.* **1977**, *6*, 357.

Contribution from the School of Chemical Sciences, University of Illinois at Urbana-Champaign, Urbana, Illinois 61801

Synthesis, Structure, and Reactivity of Organoruthenium Derivatives of Tetrathio- and Tetraselenometalates

Kevin E. Howard, Thomas B. Rauchfuss,* and Scott R. Wilson

Received October 29, 1987

We describe the preparation of a series of organoruthenium tetrathiometalates and tetraselenometalates of the general formula $(RC_5H_4)_2Ru_2L_2ME_4$ (R = H, CH_3; L = PR_3, RNC, CO; M = W, Mo; E = S, Se). The compound $Cp_2Ru_2(PPh_3)_2WS_4$ (**1**) reacts with PMe_3 to give $Cp_2Ru_2(PMe_3)_2WS_4$ and with isocyanides to give $Cp_2Ru_2(RNC)_2WS_4$ (R = *t*-Bu, Me, $C_6H_5CH_2$). Only *one* of the PPh_3 ligands in **1** is substituted by an excess of carbon monoxide to give $Cp_2Ru_2(PPh_3)(CO)WS_4$. The kinetics of the ligand substitution of **1** by *t*-BuNC was examined by using ^{1}H NMR spectroscopy. The rate of the first substitution was found to be independent of [*t*-BuNC], the first-order rate constant being 5.6×10^{-4} s^{-1}. The rate of the first substitution was found to be approximately 4 times that of the second. All of the compounds studied undergo reversible or quasi-reversible oxidations. On the basis of the measured $E_{1/2}$ values, the donor powers of the chalcogenometalates are ranked as follows: $MoSe_4^{2-} > WSe_4^{2-} > MoS_4^{2-} > WS_4^{2-}$. The compound $Cp_2Ru_2(MeNC)_2WS_4$ crystallizes in the monoclinic space group $I2/a$ with $a = 13.840$ (13) Å, $b = 12.234$ (9) Å, $c = 14.224$ (11) Å, $\beta = 105.48$ (7)°, $V = 2321$ (3) Å^3, and $Z = 4$ and refined to $R = 0.038$ and $R_w = 0.049$. The short Ru-W distances (2.870 (2) Å) and the acute Ru-S-W angles (77° average) are indicative of metal-metal bonding. The reactivity, redox properties, and structures of these compounds are discussed in the context of the donation of t_{2g} electrons on ruthenium to tungsten.

Introduction

The tetrathiometalates have been employed as ligands for transition metals for the past 20 years.[1] Interest in these coordination compounds has expanded rapidly because of evidence or assumptions that certain thiometalate complexes are structurally related to catalytic sites in both nitrogen-fixing enzymes[2-4] and industrial hydrotreating catalysts.[5] More fundamental incentives for interest in this area follow from the electronic novelty[6,7] of these complexes vis-à-vis other dithio chelates.

Tetrathiometalate complexes are derivatives of MoS_4^{2-}, WS_4^{2-}, VS_4^{3-},[8-10] and ReS_4^-.[10,11] The latter two anions have been studied only recently as have tetraselenometalate complexes.[12] The majority of tetrathiometalate complexes are of the type $L_2M'(MS_4)$[13] or $M'(MS_4)_2^Z$ [6,14,15] (many of the binary molybdenum

(1) Müller, A.; Diemann, E.; Jostes, R.; Bögge, H. *Angew. Chem., Int. Ed. Engl.* **1981**, *16*, 934.
(2) Holm, R. H. *Chem. Soc. Rev.* **1981**, *10*, 455.
(3) Coucouvanis, D. *Acc. Chem. Res.* **1981**, *14*, 201.
(4) Zumft, W. G. *Eur. J. Biochem.* **1978**, *91*, 345.
(5) Pan, W.-H.; Johnston, D. C.; McKenna, S. T.; Chianelli, R. R.; Halbert, T. R.; Hutchings, L. L.; Stiefel, E. I. *Inorg. Chim. Acta* **1985**, *97*, L17.
(6) Bowmaker, G. A.; Boyd, P. D. W.; Sorrenson, R. J.; Reed, C. A.; McDonald, J. W. *Inorg. Chem.* **1985**, *24*, 3.
(7) Bowmaker, G. A.; Boyd, P. D. W.; Campbell, G. K.; Zvagulis, M. *J. Chem. Soc., Dalton Trans.* **1986**, 1065.
(8) Kovacs, J. A.; Holm, R. H. *Inorg. Chem.* **1987**, *26*, 702, 711. Carney, M. J.; Kovacs, J. A.; Zhang, Y.-P.; Papaefthymiou, G. C.; Spartalian, K.; Frankel, R. B.; Holm, R. H. *Inorg. Chem.* **1987**, *26*, 719.
(9) Halbert, T. R.; Hutchings, L. L.; Rhodes, R.; Stiefel, E. I. *J. Am. Chem. Soc.* **1986**, *108*, 6437.
(10) Do, Y.; Simhon, E. D.; Holm, R. H. *Inorg. Chem.* **1985**, *24*, 4635.
(11) Müller, A.; Krickmeyer, E.; Bögge, H. *Angew. Chem., Int. Ed. Engl.* **1986**, *26*, 990.
(12) Wardle, R. W. M.; Chau, C.-N.; Ibers, J. A. *J. Am. Chem. Soc.* **1987**, *109*, 1859.

0020-1669/88/1327-1710$01.50/0

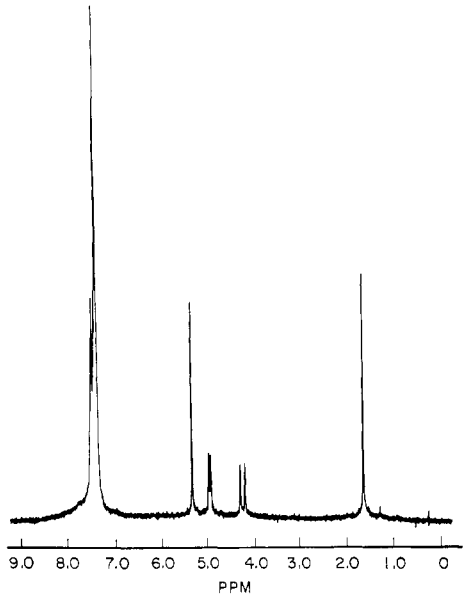

Figure 1. 200-MHz ^1H NMR spectrum of $(MeCp)_2Ru_2(PPh_3)_2WS_4$ (CD_2Cl_2).

and tungsten sulfides[15] may be viewed as members of this structural class). A second class of tetrathiometalate complexes are of the type $(M'L_n)_2(\mu\text{-}MS_4)$.[10,16]

The catalytic roles envisioned for thiomolybdates naturally leads to an interest in the substitution and addition reactions of the molybdenum sulfide clusters. In the biological context, partial success has been achieved for clusters of the type $X_3Fe_3Mo(catecholate)LS_4^{n-}$, which form adducts with a range of basic nitrogen ligands.[17] Salts of $Fe(WS_4)_2^{2-}$ bind σ donors to give the adducts $FeL_2(WS_4)_2^{2-}$.[14c] In our search for substitutionally active thiometallate clusters, we have not restricted our attention to biologically plausible components. Instead we have focused on derivatives of those metals with well-established affinity for π-acid ligands. We have found that the tetrathiometalates form robust yet reactive complexes with ruthenium, rhodium, and iridium and that these compounds are often controllably reactive.[18]

The compounds $Cp_2Ru_2(PPh_3)_2MS_4$ are particularly well-behaved and are the subject of this paper. These compounds readily undergo ligand substitution reactions at ruthenium and exhibit well-behaved electrochemistry. Both processes have been studied,

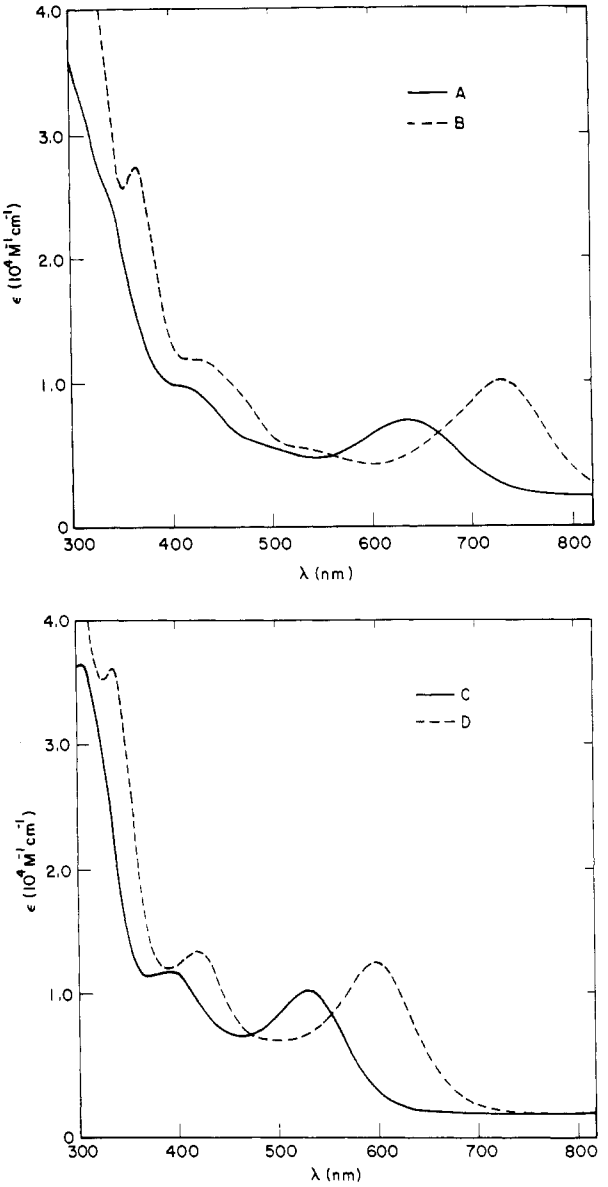

Figure 2. Visible absorption spectra for $(MeCp)_2Ru_2(PPh_3)_2ME_4$ where ME_4 = MoS_4 (a), $MoSe_4$ (b), WS_4 (c), and WSe_4 (d).

and their characterization has demonstrated the importance of long-range metal–metal interactions in this class of trimetallic complexes. Prior to our work, the only examples of organometallic tetrathiometalates were of the type $Cp_2M'MS_4$ where M and M' are either Mo or W.[19]

Results

Synthesis. Trimetallic compounds of the formula $(RCp)_2Ru_2(PPh_3)_2MS_4$ (R = H, CH_3; M = W (**1**), Mo (**2**)) are readily prepared from the reaction of 2 equiv of $(RCp)Ru(PPh_3)_2Cl$ with $(Ph_4P)_2MS_4$ in refluxing acetonitrile (eq 1). Two

$$2(RCp)Ru(PPh_3)_2Cl + (Ph_4P)_2MS_4 \rightarrow (RCp)_2Ru(PPh_3)_2MS_4 + 2PPh_3 \quad (1)$$

1 (R = H; M = W)
2 (R = H; M = Mo)

equivalents of PPh_3 are displaced in these reactions. The resulting red **1** (M = W) or green **2** (M = Mo) products were obtained as analytically pure microcrystalline precipitates, in 55–80% yields. These compounds are air-stable and were characterized by spectroscopic methods. Their ^1H NMR spectra consist of a multiplet for the phenyl groups and a singlet for the equivalent

(13) Siedel, A. R.; Hubbard, C. R.; Mighell, A. D.; Doherty, R. M.; Stewart, J. M. *Inorg. Chim. Acta* **1980**, *38*, 197.
(14) (a) $M(M'OS_3)_2^{2-}$ (M = Ni, Pd, Pt): Callahan, K. P.; Cichon, E. J. *Inorg. Chem.* **1981**, *20*, 1941. (b) $M(M'S_4)_2^{2-}$ (M = Ni, Pd, Pt): Callahan, K. P.; Piliero, P. A. *Inorg. Chem.* **1980**, *19*, 2619. (c) $Fe(WS_4)_2^{2-}$: Stremple, P.; Baenziger, N. C.; Coucouvanis, D. *J. Am. Chem. Soc.* **1981**, *103*, 4601. (d) $Co(WS_4)_2^{2-/3-}$: Müller, A.; Hellmann, W.; Schimanski, U.; Jostes, R.; Newton, W. E. *Z. Naturforsch., B: Anorg. Chem., Org. Chem.* **1983**, *38*, 528. Müller, A.; Jostes, R.; Flemming, V.; Potthast, R. *Inorg. Chim. Acta* **1980**, *44*, L33.
(15) (a) $Mo_2S_6^{2-}$, $Mo_2S_7^{2-}$, and $Mo_2S_9^{2-}$: Coucouvanis, D.; Hadjikyriacou, A. *Inorg. Chem.* **1987**, *26*, 1. (b) $W_4S_{12}^{2-}$: Secheresse, F.; LeFebvre, J.; Daran, J. C.; Jeannin, Y. *Inorg. Chem.* **1982**, *21*, 1311. (c) $W_3S_9^{2-}$: Cohen, S. A.; Stiefel, E. I. *Inorg. Chem.* **1985**, *24*, 4657. (d) $W_3S_8^{2-}$: Bhaduri, S.; Ibers, J. A. *Inorg. Chem.* **1986**, *25*, 3 (we have had difficulty reproducing this synthesis).
(16) (a) $(FeCl_2)_2WS_4^{2-}$: Coucouvanis, D.; Simhon, E. D.; Stremple, P.; Ryan, M.; Swenson, D.; Baenziger, N. C.; Simopoulos, A.; Papaefthymiou, V.; Kostikas, A.; Petrouleas, V. *Inorg. Chem.* **1984**, *23*, 741. (b) $Au_2(PPh_3)_nMoS_4$ (*n* = 2, 3): Charnock, J. M.; Bristow, S.; Nicholson, J. R.; Garner, C. D.; Clegg, W. *J. Chem. Soc., Dalton Trans.* **1987**, 303. (c) $Au_2(PEt_3)_2MoS_4$: Kinsch, E. M.; Stephan, D. W. *Inorg. Chim. Acta* **1985**, *96*, L87. (d) For developments in copper systems see: Manoli, J. M.; Potvin, C.; Secheresse, F.; Marzak, S. *J. Chem. Soc., Chem. Commun.* **1986**, 1557.
(17) Palermo, R. E.; Singh, R.; Bashkin, J. K.; Holm, R. H. *J. Am. Chem. Soc.* **1984**, *106*, 2600, and references therein. Holm, R. H.; Simhon, E. D. In *Molybdenum Enzymes*: Spiro, T. G., Ed.; Wiley Interscience: New York, 1985; Chapter 1.
(18) Howard, K. E.; Rauchfuss, T. B.; Rheingold, A. L. *J. Am. Chem. Soc.* **1986**, *108*, 297.
(19) Adam, G. J. S.; Green, M. L. H. *J. Organomet. Chem.* **1981**, *208*, 299. Ruffing, C. J.; Rauchfuss, T. B. *Organometallics* **1982**, *1*, 400.

Cp groups. The chirality of the new compounds is indicated by the ^{1}H NMR spectra of their MeCp derivatives, where four multiplets of equal intensity are observed for the C_5H_4Me protons (Figure 1). The infrared spectra of these species show moderately strong absorptions at 448 cm^{-1} (ν_{W-S}). The compounds exhibit molecular ion envelopes (MH^+) in their fast-atom-bombardment mass spectra. Finally, these compounds show an intense absorption in the visible region with λ_{max} = 530 nm for **1** and λ_{max} = 638 nm for **2** (Figure 2).

In order to examine the corresponding tetraselenometalate complexes, we prepared organic soluble salts of $MoSe_4^{2-}$ and WSe_4^{2-}. Adaptation of Stiefel's MoS_4^{2-} synthesis[20] gave $(NH_4)_2MoSe_4$[21] in high yield. This material underwent smooth metathesis with Ph_4PCl to give the well-behaved, turquoise $(Ph_4P)_2MoSe_4$. Salts of WSe_4^{2-} were prepared by the reaction of $W(t\text{-NBu})_2(t\text{-NHBu})_2$[22] with H_2Se in CH_2Cl_2 (eq 2). The

$$W(t\text{-NBu})_2(t\text{-NHBu})_2 + 4H_2Se \rightarrow [t\text{-BuNH}_3]_2WSe_4 + 2t\text{-BuNH}_2 \quad (2)$$

red-brown precipitate obtained crystallized nicely to give bright red crystalline $[t\text{-BuNH}_3]_2WSe_4$ in good yield. This methodology is very convenient since it requires only stoichiometric quantities of H_2Se, it affords an organic soluble salt, and it is suited for Schlenk techniques. Attempts to prepare $[t\text{-BuNH}_3]_2WTe_4$ by this method failed to give soluble compounds.

The $MoSe_4^{2-}$ and WSe_4^{2-} complexes $(MeCp)_2Ru_2(PPh_3)_2MSe_4$ were prepared in a manner analogous to the sulfur derivatives. The tetraselenometalate complexes are somewhat air- and moisture-sensitive but can readily be obtained in analytically pure form by using standard Schlenk techniques. Both derivatives are quite soluble in CH_2Cl_2 and $CHCl_3$ and have been characterized spectroscopically and electrochemically. Changing E from S to Se in $(MeCp)_2Ru_2(PPh_3)_2ME_4$ does not lead to appreciable changes in the ^{1}H NMR resonances of the coligands. Similarly, only small changes (~2 ppm) are observed in the ^{31}P NMR spectra. The visible absorption maxima are red-shifted 60–80 nm in the selenium compounds compared with the maxima in sulfides (Figure 2). These Ru–Mo–Se and Ru–W–Se compounds represent the first reported heterometallic tetraselenometalate complexes.

Substitution Reactions. Complexes **1** and **2** undergo a variety of substitution reactions (eq 3). For example treatment of so-

$$Cp_2Ru_2(PPh_3)_2MS_4 + 2L \rightarrow Cp_2Ru_2L_2MS_4 + 2PPh_3 \quad (3)$$

lutions of $(RC_5H_4)_2Ru_2(PPh_3)_2WS_4$ with PMe_3 gave the bright red bis(trimethylphosphine) derivative in good yield. The ^{1}H NMR chemical shift for the C_5H_5 resonances is shifted 0.30 ppm downfield when PMe_3 is substituted for both triphenylphosphine ligands in $Cp_2Ru_2(PPh_3)_2WS_4$. The ν_{W-S} value decreases by 12 cm^{-1} from 448 to 436 cm^{-1} upon substitution of PPh_3 by PMe_3. The compound $(MeCp)_2Ru_2(PMe_3)_2WS_4$ exhibits high solubility in pentane.

Treatment of **1** or its MeCp analogue with an excess of carbon monoxide gave the monocarbonyl derivatives $(RC_5H_4)_2Ru_2(PPh_3)(CO)WS_4$ in very high yield (eq 4). Purified samples of

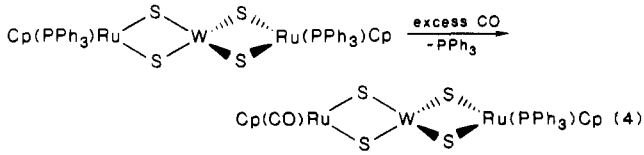

(4)

$Cp_2Ru_2(PPh_3)(CO)WS_4$ resisted further carbonylation. Characteristic ν_{CO} bands are observed at 1977 and 1971 cm^{-1} for the Cp and MeCp derivatives, respectively. For comparison the ν_{CO} value for $CpRu(PPh_3)(CO)SH$[23] is 1948 cm^{-1}. The ^{1}H NMR spectrum of the monocarbonyl shows two Cp resonances, both

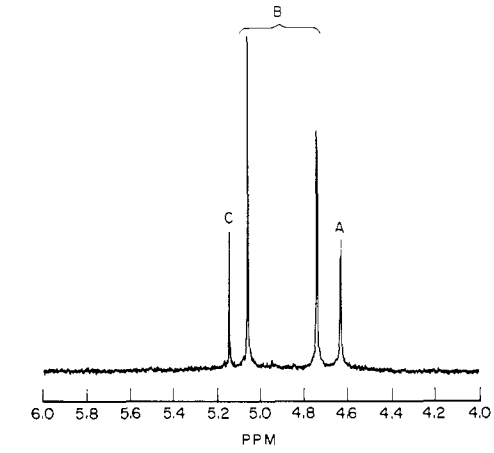

Figure 3. 200-MHz ^{1}H NMR spectrum, showing the Cp region, of a mixture containing $Cp_2Ru_2(PPh_3)_{2-x}(t\text{-BuNC})_xWS_4$ where x = 0 (A), 1 (B), and 2 (C).

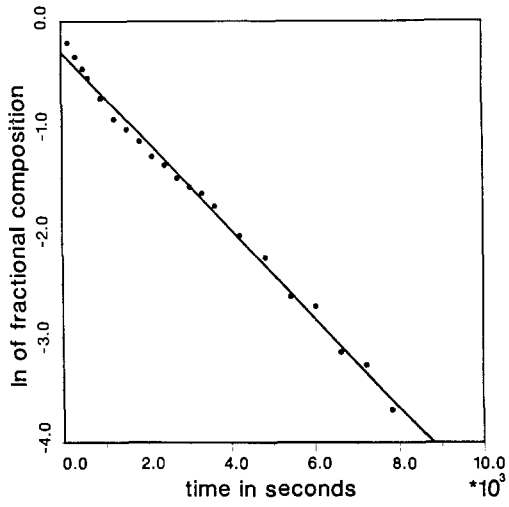

Figure 4. Plot of ln [A] vs t, where A = $Cp_2Ru_2(PPh_3)_2WS_4$, for $Cp_2Ru_2(PPh_3)_2WS_4$ + 6t-BuNC.

of which are well separated from that of **1**. Despite its low symmetry, the monocarbonyl exists only as a single enantiomeric pair. The low symmetry of the monocarbonyl complex is indicated by the 200-MHz ^{1}H NMR spectrum of the MeCp derivative, which shows two methyl resonances and three MeC_5H_4 resonances.

Isocyanides react readily with solutions of **1**. Treatment of dichloromethane solutions of **1** with MeNC, t-BuNC, or benzyl isocyanide results in substitution at *both* ruthenium centers, giving bright red, air-stable crystalline products in 53–90% yield. The solution IR spectra for $Cp_2Ru_2(RNC)_2WS_4$ exhibit single ν_{NC} bands at 2160 (R = Me), 2126 (R = t-Bu), and 2139 cm^{-1} (R = Bz). For comparison, ν_{NC} for the free isocyanides (measured as CH_2Cl_2 solutions) are 2167 (MeNC), 2140 (t-BuNC), and 2154 cm^{-1} (BzNC).[24]

Substitution Kinetics. The substitution of **1** by t-BuNC was monitored by using ^{1}H NMR spectroscopy. We observe a steady decrease in **1**, the formation and subsequent decay of $Cp_2Ru_2(PPh_3)(t\text{-BuNC})WS_4$, and finally the formation of $Cp_2Ru_2(t\text{-BuNC})_2WS_4$ (eq 5). The concentrations of each of the above

$$Cp_2Ru_2(PPh_3)_2WS_4 \xrightarrow{k_1} Cp_2Ru_2(PPh_3)(t\text{-BuNC})WS_4 \xrightarrow{k_2} Cp_2Ru_2(t\text{-BuNC})_2WS_4 \quad (5)$$

species were determined by integrating the Cp region of the ^{1}H NMR spectra. Figure 3 shows the Cp region of the ^{1}H NMR spectrum at an intermediate reaction time, where all three species

(20) Pan, W.-H.; Leonowicz, M. E.; Stiefel, E. I. *Inorg. Chem.* **1983**, *22*, 672.
(21) Müller, A.; Krebs, B.; Diemann, E. *Angew. Chem., Int. Ed. Engl.* **1967**, *6*, 257.
(22) Nugent, W. A.; Harlow, R. L. *Inorg. Chem.* **1980**, *19*, 777.
(23) Amarasekera, J.; Howard, K. E.; Rauchfuss, T. B.; Wilson, S. R., unpublished results.
(24) For studies of $CpRu(MeNC)_2Cl$ and $CpRu(t\text{-BuNC})_2Cl$, see: Albers, M. O.; Robinson, D. J.; Shaver, A.; Singleton, E. *Organometallics* **1986**, *5*, 2199.

Table I. Cyclic Voltammetry Data for $(RC_5H_4)_2Ru_2L_2ME_4$ Complexes

compd	$E_{1/2}$,[a] mV	ΔE_p, mV	i_{pa}/i_{pc}
$Cp_2Ru_2(PPh_3)_2WS_4$	+527	67	1.18
$(MeCp)_2Ru_2(PPh_3)_2WS_4$	+482	70	1.31
$Cp_2Ru_2(PMe_3)_2WS_4$	+459	63	0.84
$(MeCp)_2Ru_2(PMe_3)_2WS_4$	+318	60	0.86
$Cp_2Ru_2(PPh_3)_2MoS_4$	+479	59	1.05
$(MeCp)_2Ru_2(PPh_3)_2MoS_4$	+403	57	1.03
$(MeCp)_2Ru_2(PPh_3)_2MoSe_4$	+314	67	0.96
$(MeCp)_2Ru_2(PPh_3)_2WSe_4$	+373	67	1.05
$Cp_2Ru_2(PPh_3)(CO)WS_4$	+724	59	1.51
$(MeCp)_2Ru_2(PPh_3)(CO)WS_4$	+662	91	1.49
$Cp_2Ru_2(t\text{-BuNC})_2WS_4$	+571	87	1.73
$Cp_2Ru_2(CNCH_2C_6H_5)_2WS_4$	+630	77	2.77
$CpRu(PPh_3)_2Cl$	+590	70	0.80
$(MeCp)Ru(PPh_3)_2Cl$	+542	61	0.91
$CpRu(PMe_3)_2Cl$	+387	58	1.00

[a] Versus Ag/AgCl in CH_2Cl_2 solution containing 0.1 M Bu_4NPF_6.

are present. The C_5H_5 resonance for the ruthenium center bearing the phosphine shows a small $J(^{31}P, ^1H)$ coupling. The rate of the substitution process was observed to be independent of [*t*-BuNC]. This indicates that the substitution mechanism is dissociative. The plots of −ln [**1**] vs *t* were linear, $k_1 = 5.6 \times 10^{-4}$ s^{-1} (Figure 4). We were not able to satisfactorily model the kinetics of the entire substitution process. Using an internal standard, we demonstrated that mass balance was obeyed; i.e., [**1**] + $[Cp_2Ru_2(PPh_3)(t\text{-BuNC})WS_4]$ + $[Cp_2Ru_2(t\text{-BuNC})_2WS_4]$ = constant. The first substitution process is approximately *four* times greater than the second substitution after correcting for statistical effects. The replacement of one triphenylphosphine on the Ru_2WS_4 core by an isocyanide does not strongly inhibit the second substitution process in contrast to the case for carbon monoxide. This observation is in accord with the ν_{NC} data, which indicate that the isocyanides are not functioning as π-acceptors in these complexes.

Electrochemistry. The $(RC_5H_4)_2Ru_2L_2MS_4$ complexes all undergo single one-electron oxidations, which were investigated by cyclic voltammetry. On the basis of the current ratios i_{pa}/i_{pc}, these redox couples are either reversible or, in the case of the isocyanide complexes, quasi-reversible. Comparison of the $E_{1/2}$ values for the various complexes provides an indication of the donor/acceptor properties of the subunits in the $(RCp)_2Ru_2L_2ME_4$ complexes (Table I). For comparative purposes we measured the $E_{1/2}$ values for $CpRu(PPh_3)_2Cl$ (590 mV) and $(MeCp)Ru(PPh_3)_2Cl$ (542 mV).

Simply substituting the more electron-donating MeCp ligand for Cp in $Cp_2Ru_2(PPh_3)_2WS_4$ shifts the $E_{1/2}$ value from +527 mV (versus Ag/AgCl) (Cp) to +482 mV (MeCp). A more dramatic effect is seen when one PPh_3 ligand has been substituted by CO. This ligand substitution results in a 197-mV shift of $E_{1/2}$; i.e., the monocarbonyl species is considerably more difficult to oxidize than the bis(triphenylphosphine) compound **1**. Translated into an equilibrium constant, we calculate $K_{eq} \approx 2000$ for eq 6. The cyclic

$$Cp_2Ru_2(PPh_3)_2WS_4 + [Cp_2Ru_2(PPh_3)(CO)WS_4]^+ \overset{K_{eq}}{\rightleftharpoons} [Cp_2Ru_2(PPh_3)_2WS_4]^+ + Cp_2Ru_2(PPh_3)(CO)WS_4 \quad (6)$$

voltammetry data show that the $E_{1/2}$ values for $Cp_2Ru_2(RNC)_2WS_4$, where R = *t*-Bu and $C_6H_5CH_2$, lie between those of $Cp_2Ru_2(PPh_3)_2WS_4$ and $Cp_2Ru_2(PPh_3)(CO)WS_4$. The most easily oxidized WS_4-containing species is the trimethylphosphine complex $Cp_2Ru_2(PMe_3)_2WS_4$. On the basis of the $E_{1/2}$ values, we observed the expected ranking of the coligands in terms of their donor properties; i.e., $PMe_3 > PPh_3 > RNC > CO$. The compounds $(MeCp)_2Ru_2(PPh_3)_2ME_4$ (M = Mo, W.; E = S, Se) all exhibited well-behaved electrochemistry (the MeCp derivatives were chosen for solubility purposes). The compound $(MeCp)_2Ru_2(PPh_3)_2MoSe_4$ is the most reducing member of the series. On the basis of our results the following ranking of the donor properties of the tetrachalcogenometalates is observed: $WS_4^{2-} < MoS_4^{2-} < WSe_4^{2-} < MoSe_4^{2-}$. It appears that effects of the chalcogen ($\Delta E_{1/2} \approx 90$ mV) outweigh the effects of the central metal ($\Delta E_{1/2} \approx 60$–80 mV). The effects of substituents, i.e., MeCp vs Cp, Mo vs W, and S vs Se, on the redox couples appear to be reasonably additive.

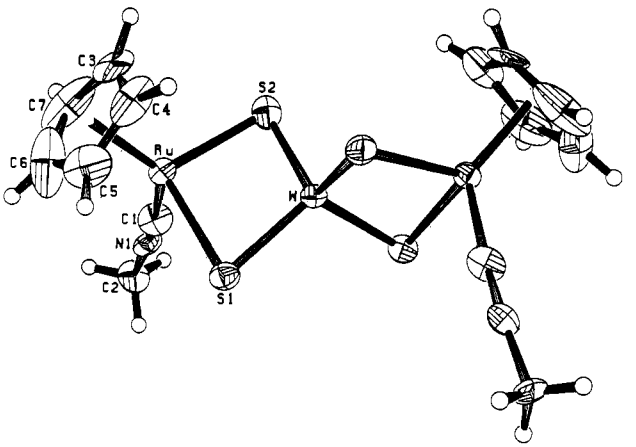

Figure 5. Structure of $Cp_2Ru_2(MeNC)_2WS_4$ with non-hydrogen thermal ellipsoids drawn at the 35% probability level.

Table II. Selected Bond Lengths (Å) and Angles (deg) for $Cp_2Ru_2(MeNC)_2WS_4 \cdot CH_2Cl_2$

W–Ru	2.870 (2)	W–S1	2.212 (6)
Ru–S1	2.394 (6)	W–S2	2.212 (6)
Ru–S2	2.377 (6)	Ru–C1	1.90 (3)
N1–C1	1.20 (3)	N1–C2	1.47 (3)
Ru–C3	2.22 (3)	Ru–C4	2.25 (4)
C3–C4	1.28 (6)	Ru–C5	2.18 (3)
C4–C5	1.40 (6)	Ru–C6	2.17 (4)
C5–C6	1.37 (8)	Ru–C7	2.13 (5)
C3–C7	1.36 (7)	C6–C7	1.30 (7)
Ru–CP[a]	1.89 (4)	C1A–C8[b]	1.6 (1)
C1B–C8[b]	1.9 (1)		
Ru–W–Ru[c]	162.74 (7)	Ru–W–S1	54.4 (2)
Ru–W–S1[c]	139.0 (2)	Ru–W–S2	53.9 (2)
Ru–W–S2[c]	114.9 (2)	S1–W–S1[c]	110.0 (2)
S1–W–S2	106.0 (2)	S1–W–S2[c]	111.4 (2)
S2–W–S2[c]	112.1 (2)	W–Ru–S1	48.7 (1)
W–Ru–S2	48.8 (1)	W–Ru–C1	98.9 (8)
S1–Ru–S2	95.6 (2)	S1–Ru–C1	87.7 (8)
S2–Ru–C1	89.7 (7)	S2–Ru–C3	92.8 (9)
S2–Ru–CP	116 (1)	C1–Ru–C3	133 (1)
C1–Ru–CP	135 (2)	C3–Ru–C4	33 (1)
W–S1–Ru	77.0 (2)	W–S2–Ru	77.3 (2)
C1–N1–C2	175 (2)	Ru–C1–N1	174 (2)
C4–C3–C7	115 (4)	C3–C4–C5	102 (4)
C4–C5–C6	109 (4)	C5–C6–C7	109 (5)
C3–C7–C6	104 (4)	C1A–C8–C1B	109 (6)

[a] CP = cyclopentadienyl centroid. [b] CH_2Cl_2 was disordered about the 2-fold axis. [c] Equivalent position about 2-fold axis.

Crystal Structure of $Cp_2Ru_2(MeNC)_2WS_4$. Crystallographic twofold symmetry is imposed on the roughly tetrahedral WS_4 unit with one unique pair of sulfur atoms bridging to a ruthenium atom (Figure 5). Bond distances and angles are presented in Table II. Each ruthenium atom is bound to a cyclopentadienyl ring, a methyl isocyanide group, and two sulfur atoms of the WS_4. The W–S distances (2.22 Å) are similar to those in $WS_4Rh_2(COD)_2$ (2.20 Å average)[18] but are longer than those in $(NH_4)_2WS_4$ (2.165 Å).[25] The relatively short W–Ru distance of 2.870 (2) Å and the acute Ru–S–W angles of 77.0 (2) and 77.3 (2)° also indicate metal–metal bonding. The Ru–S distances at 2.377 (6) and 2.394 (6) Å are typical; in comparison, the Ru–S bonds in $[CpRu(PPh_3)_2(n\text{-PrSH})]BF_4$[26] and the S-bound thiophene complex $[(C_5H_4CH_2\text{-}2\text{-}C_4H_3S)Ru(PPh_3)_2](BF_4)$[27] are 2.38 and 2.41 Å, respectively. Sulfur ligands can engage in strong π-bonding with

(25) Sasvari, K. *Acta Crystallogr.* **1963**, *16*, 719.
(26) Draganjac, M. E.; Rauchfuss, T. B.; Wilson, S. R., unpublished results.
(27) Draganjac, M. E.; Rauchfuss, T. B.; Ruffing, C. J.; Wilson, S. R. *Organometallics* **1985**, *4*, 1909.

ruthenium, but in such electron deficient complexes the Ru–S distances are short, viz. $[CpRu(PMe_3)]_2(\mu\text{-}S_2)[SbF_6]_2$ (2.18 Å)[28] and $(C_5Me_4Et)_2Ru_2S_4$ (2.20 Å).[29]

Discussion

The tetrathio and tetraseleno derivatives of molybdenum and tungsten were found to readily form organometallic complexes of the type $Cp_2Ru_2L_2ME_4$. As was desired, these compounds undergo ready substitution of the two unidentate ligands on the ruthenium atoms. The two ruthenium centers are electronically strongly coupled despite the fact that they are 5.68 Å apart. Communication between the ruthenium centers is evidenced by the fact that only one of the two triphenylphosphine ligands can be substituted by carbon monoxide. In contrast, both phosphines can be readily substituted by good Lewis bases. The strong coupling between the two ruthenium centers is also signaled by the fact that all of our trimetallic complexes undergo only a single oxidation whereas two oxidations would be expected if the ruthenium centers were not electronically coupled. Neutral ruthenium complexes of the type $CpRu(PR_3)_2X$ generally exhibit reversible redox couples within a few hundred millivolts of Ag/AgCl. Our results are consistent with mounting evidence that WS_4^{2-} is a strong electron acceptor ligand as supported by studies on the $Fe(MS_4)_2^{2-/3-}$ and $Co(MS_4)_2^{2-/3-}$ systems.[6,14c,d]

The crystal structure of $Cp_2Ru_2(MeNC)_2WS_4$ indicates tungsten–ruthenium bonding. The Ru–S–W angles are acute, and the intermetallic distances are completely consistent with direct metal–metal bonding. The W–S distances are 0.05 Å longer than in $(NH_4)_2WS_4$. In comparison with a number of recent structural studies, the Ru–S distances appear perfectly normal and Ru–S π-bonding is not indicated. We propose that the Ru–W bonding compensates for the W–S π-bonding sacrificed upon complexation of WS_4^{2-} to the ruthenium centers. This compensation hypothesis leads one to predict that WS_4^{2-} and MoS_4^{2-} would form stable complexes with transition metals whose d-electron configuration allows them to participate in dative M to W(Mo) bonding. As such, metals with the $(t_{2g})^6$ configuration are ideal hosts for tetrathiometalate ligands.

A recent paper has discussed the bonding in MoS_4^{2-} in terms of a HOMO of Mo–S π character and a metal-centered LUMO.[30] These conclusions are compatible with the bond compensation hypothesis described above. The Mo–S π-bonds would necessarily be weakened by coordination of the sulfur centers to a second metal. The metal-based LUMO of MoS_4^{2-} is of d_{z^2} character, which would be suitably orientated for overlap with one of the filled t_{2g} orbitals on each of the pseudooctahedral ruthenium(II) centers. A three-centered, four-electron interaction can be envisioned. Such a trimetal bonding network would be expected to be very sensitive to the oxidation state of the entire unit, hence the observation of a single redox couple in the Ru_2ME_4 compounds studied in this paper. The t_{2g} electrons on ruthenium are, of course, also of suitable symmetry for π-bonding to π-acid ligands. Thus in $Cp_2Ru_2(PPh_3)(CO)WS_4$, there exists a competitive relationship between Ru–CO π-bonding and the Ru–W σ-bonding. This reasoning explains why $Cp_2Ru_2(PPh_3)_2WS_4$ undergoes double substitution by good donor ligands (PMe_3, RNC) but only single substitution by CO.

Experimental Section

Materials and Methods. All compounds described herein are air-stable, except for the $MoSe_4^{2-}$ and WSe_4^{2-} complexes; however, all reactions were carried out under a nitrogen atmosphere. Acetonitrile was distilled from calcium hydride under nitrogen. Methylene chloride was distilled from P_4O_{10} under nitrogen. All other solvents were reagent grade and were used without further purification. $(MeCp)Ru(PPh_3)_2Cl$,[31] $CpRu(PPh_3)_2Cl$,[31] $(NH_4)_2WS_4$,[20] $W(t\text{-}NBu)_2(t\text{-}NHBu)_2$,[22] and $(NH_4)_2MoS_4$[20] were prepared by literature methods. $(Ph_4P)_2WS_4$ and $(Ph_4P)_2MoS_4$ were prepared by metathesis of the ammonium salt with tetraphenylphosphonium chloride in water.[32] H_2Se was purchased from Matheson.

^1H NMR spectra were recorded on a Varian XL-200 spectrometer by using $CDCl_3$ (0.03% TMS) solvent and are reported in ppm versus TMS. $^{31}P\{^1H\}$ NMR spectra were recorded on a home-built 250 MHz instrument operating at 101.3 MHz with a Nicolet 1280 data system. ^{31}P NMR spectra were measured on CH_2Cl_2 solutions with chemical shifts reported in ppm versus an external standard at 85% H_3PO_4. UV–visible spectra were recorded on a Varian 2300 spectrophotometer. Infrared spectra were recorded on Nicolet MX-S FT-IR and Perkin-Elmer 1750 FT-IR spectrophotometers. Elemental analyses were performed by the University of Illinois microanalytical laboratory. Fast-atom-bombardment mass spectra were measured on a ZAB-SE mass spectrometer by the University of Illinois Mass Spectrometry lab.

Electrochemical measurements were carried out on a BAS-100 electrochemical analyzer on CH_2Cl_2 solutions, which were 10^{-3} M in compound and 0.1 M in $[NBu_4][PF_6]$, with a Pt disk electrode. $E_{1/2}$ values are reported versus Ag/AgCl. Under these conditions the ferrocene/ferrocenium couple is at +481 mV. The scan rates were 200 mV/s except for the studies on the isocyanide complexes where a 50 mV/s scan rate was used.

$Cp_2Ru_2(PPh_3)_2WS_4$ (1). A 1.00-g (1.38-mmol) sample of $CpRu(PPh_3)_2Cl$ and 0.638 g (0.69 mmol) of $(Ph_4P)_2WS_4$ were heated in 150 mL of refluxing CH_3CN for 18 h. The red crystalline precipitate was washed with 60 mL of CH_3CN and dried in vacuo. The compound may be recrystallized from CH_2Cl_2/CH_3CN although the crude product was usually obtained analytically pure. The yield was 0.60 g (74%). Anal. Calcd for $C_{46}H_{40}P_2Ru_2S_4W$: C, 47.26; H, 3.45; S, 10.97; P, 5.30. Found: C, 47.09; H, 3.63; S, 11.21; P, 5.19. ^1H NMR: 7.50 (m, 30 H); 4.71 (s, 10 H). ^{31}P NMR: 48.7 (s). UV–visible (CH_2Cl_2 solution): λ_{max} = 530 nm; ϵ = 5800 M^{-1} cm^{-1}. FABMS: 1170, $(M - H)^+$. IR (KI): 448 cm^{-1}.

$(MeCp)_2Ru_2(PPh_3)_2WS_4$. In a procedure analogous to that above, 0.250 g (0.331 mmol) of $(MeCp)Ru(PPh_3)_2Cl$ and 0.163 g (0.165 mmol) of $(Ph_4P)_2WS_4$ gave 0.110 g (56%) of red microcrystalline product. Anal. Calcd for $C_{48}H_{44}P_2Ru_2S_4W$: C, 48.16; H, 3.71; S, 10.71; P, 5.17. Found: C, 47.99; H, 3.74; S, 10.49; P, 5.24. ^1H NMR: 7.40 (m, 30 H); 4.90 (m, 4 H); 4.24 (d, 4 H); 1.60 (d, 6 H). ^1H NMR (CD_2Cl_2): 7.40 (m, 30 H); 4.94 (d, 2 H); 4.90 (d, 2 H); 4.26 (s, 2 H); 4.15 (s, 2 H); 1.59 (s, 6 H). ^{31}P NMR: 50.3 (s). IR (KI): 448 cm^{-1}.

$Cp_2Ru_2(PPh_3)_2MoS_4$. This compound was obtained as a green microcrystalline solid in 80% yield by using the Ru_2WS_4 procedure. Anal. Calcd for $C_{46}H_{40}MoP_2Ru_2S_4$: C, 51.10; H, 3.73. Found: C, 50.44; H, 3.99. ^1H NMR: 7.50 (m, 30 H); 4.78 (s, 10 H). ^{31}P NMR: 49.6 (s). UV–visible (CH_2Cl_2 solution): λ_{max} = 638 nm; ϵ = 5540 M^{-1} cm^{-1}. FABMS: 1082 $(M - H)^+$. IR (KI): 456 cm^{-1}. $(MeCp)_2Ru_2(PPh_3)_2MoS_4$ was prepared in the same manner in 79% yield. ^1H NMR: 7.30 (m, 30 H); 5.15 (s, 4 H); 5.15 (s, 4 H); 4.32 (d, 4 H); 1.56 (s, 6 H). ^{31}P NMR: 51.0 (s). IR (KI): 456 cm^{-1}.

$Cp_2Ru_2(PMe_3)_2WS_4$. A solution of $Cp_2Ru_2(PPh_3)_2WS_4$, 0.117 g (0.10 mmol), in 40 mL of CH_2Cl_2 was treated with 41 μL (0.40 mmol) of PMe_3. After being stirred overnight at ambient temperatures, the solution was diluted with 25 mL of hexane and concentrated to give 0.063 g of the deep red crystalline product (79% yield). Anal. Calcd for $C_{16}H_{28}P_2Ru_2S_4W$: C, 24.09; H, 3.54. Found: C, 24.91; H, 3.34. ^1H NMR: 5.00 (s, 10 H); 1,24 (d, 18 H), J_{HP} = 9.8 Hz. ^{31}P NMR: 7.4 (s). The MeCp derivative was prepared in an analogous manner, although the yield was only 30% due to its extremely high solubility. Samples of this compound always contained small amounts of PPh_3. ^1H NMR: 5.22 (m, 4 H); 4.60 (m, 4 H); 1.76 (s, 6 H); 1.27 (d, 18 H), J_{HP} = 10.0 Hz.

$Cp_2Ru_2(PPh_3)(CO)WS_4$. A solution of $Cp_2Ru_2(PPh_3)_2WS_4$, 0.050 g (0.043 mmol), in 20 mL of CH_2Cl_2 was purged with CO for 1 h. Hexane (5 mL) was added, and the solution volume was reduced by evaporation using a stream of CO. The yield of the bright red microcrystalline product is essentially quantitative. Anal. Calcd for $C_{29}H_{25}OPRu_2S_4W$: C, 37.26; H, 2.70. Found: C, 37.72; H, 2.98. ^1H NMR: 7.30 (m, 15 H); 5.43 (s, 5 H); 4.83 (s, 5 H). ^{31}P NMR: 49.8 (s) IR (CH_2Cl_2): ν_{CO} = 1977 cm^{-1}. $(MeCp)_2Ru_2(PPh_3)(CO)WS_4$ was prepared similarly. ^1H NMR (CD_2Cl_2): 7.30 (m, 15 H); 5.63 (s, 2 H); 5.03 (br, 4 H); 4.36 (s, 2 H); 1.85 (s, 3 H); 1.68 (s, 3 H). IR (CH_2Cl_2): ν_{CO} = 1971 cm^{-1}.

Further treatment of $Cp_2Ru_2(PPh_3)(CO)WS_4$ with a constant CO purge in CH_2Cl_2, for 8 h, gave no indication of any further carbonylated

(28) Amarasekera, J.; Rauchfuss, T. B.; Wilson, S. R. *Inorg. Chem.* **1987**, *26*, 3328. See also: Amarasekera, J.; Rauchfuss, T. B.; Rheingold, A. L. *Inorg. Chem.* **1987**, *26*, 2017.
(29) Rauchfuss, T. B.; Rodgers, D. P. S.; Wilson, S. R. *J. Am. Chem. Soc.* **1986**, *108*, 3114.
(30) Bernholc, J.; Stiefel, E. I. *Inorg. Chem.* **1985**, *24*, 1323.
(31) Bruce, M. I.; Windsor, N. J. *Aust. J. Chem.* **1977**, *30*, 1601.
(32) For details of the metathesis of $(NH_4)_2MS_4$ with Ph_4PCl, see: Stremple, Phillip P. Ph.D. Dissertation, University of Iowa, 1983. Hanewald, V. K.; Gattow, G. *Z. Anorg. Allg. Chem.* **1981**, *476*, 159. For the original description of $(NH_4)_2WSe_4$, see: Lehner, V.; Fruehan, A. J. *J. Am. Chem. Soc.* **1927**, *49*, 3076.

Table III. Summary of Crystal Data, Intensity Data Collection, and Structure Refinement Results for $Cp_2Ru_2(MeNC)_2WS_4 \cdot H_2CCl_2$

formula	$WRu_2Cl_2S_4N_2C_{15}H_{18}$
mol wt	811.46
a, Å	13.840 (13)
b, Å	12.234 (9)
c, Å	14.224 (11)
β, deg	105.48 (7)
cryst syst	monoclinic
space group	$I2/a$
V, Å^3	2321 (3)
Z	4
ρ_{calcd}, g/cm^3	2.322
cryst dimens, mm	0.1 × 0.1 × 0.8
radiation	Mo K$\bar{\alpha}$; = 0.710 73 Å
linear abs coeff (μ), cm^{-1}	68.96
transmissn factors (max, min)	0.677–0.575
scan rate, deg/min	variable, 20–2
data collcd	$3.0° < 2\theta < 36.0°$ ($\pm h,+k,+l$)
no. of tot reflcns (no. of unique reflcns; internal consistency)	942 (799; R_i = 0.038)
obsd reflcns ($I > 2.58\sigma(I)$)	662
$R = \sum\|\|F_o\| - \|F_c\|\|/\sum\|F_o\|$	0.038
$R_w = (\sum w(\|F_o\| - \|F_c\|)^2/\sum w\|F_o\|^2)^{1/2}$	0.049

Table IV. Atomic Coordinates for Non-Hydrogen Atoms

	x/a	y/b	z/c
W	0.25	0.0135 (1)	0.0
Ru	0.1080 (1)	0.0487 (1)	−0.1854 (1)
C1A	0.195 (2)	0.426 (2)	0.019 (2)
C1B	0.396 (2)	0.424 (2)	0.010 (1)
S1	0.1181 (4)	−0.0903 (5)	−0.0647 (4)
S2	0.2741 (4)	0.1144 (5)	−0.1208 (4)
N1	0.186 (1)	−0.116 (1)	−0.314 (1)
C1	0.157 (2)	−0.056 (2)	−0.260 (2)
C2	0.212 (2)	−0.194 (2)	−0.382 (1)
C3	0.046 (2)	0.216 (2)	−0.218 (4)
C4	0.016 (3)	0.184 (4)	−0.144 (2)
C5	−0.043 (2)	0.094 (4)	−0.183 (4)
C6	−0.042 (3)	0.080 (5)	−0.278 (3)
C7	0.020 (4)	0.150 (5)	−0.298 (4)
C8	0.266 (9)	0.377 (8)	−0.044 (8)

species either by IR or UV–vis spectra of the reaction mixture or a ^{1}H NMR spectrum of the isolated compound. Similarly, treatment of $Cp_2Ru_2(PPh_3)(CO)WS_4$ with 500 psi of CO for 4 h led to no further carbonylation.

$Cp_2Ru_2(RNC)_2WS_4$ (R = Me, *t*-Bu, Bz). In a typical synthesis, a solution of $Cp_2Ru_2(PPh_3)_2WS_4$, 0.150 g (0.128 mmol) in 25 mL of CH_2Cl_2, was treated with 58 μL (0.513 mmol) of *t*-BuNC. After being stirred overnight, this solution was diluted with 5 mL of hexane and concentrated, giving red crystals that were washed with cold pentane. The isolated yields of these syntheses range from 53% (*t*-BuNC) to 90% (MeNC). The product was washed with cold pentane. Anal. Calcd for $C_{20}H_{28}N_2Ru_2S_4W$ (R = *t*-Bu): C, 29.63; H, 3.48; N, 3.46; S, 15.82. Found: C, 30.23; H, 3.46; N, 3.32; S, 16.47. ^{1}H NMR: 5.22 (s, 10 H); 1.30 (s, 18 H). Anal. Calcd for $C_{26}H_{24}N_2Ru_2S_4W$ (R = $C_6H_5CH_2$): C, 35.50; H, 2.75; N, 3.18. Found: C, 34.74; H, 2.73; N, 3.18. ^{1}H NMR: 7.30 (m, 10 H); 5.27 (s, 10 H); 4.75 (s, 4 H). The CH_3NC complex was not isolated in pure form due to fractional loss of CH_3NC. Anal. Calcd for $C_{14}H_{16}N_2Ru_2S_4W$ (R = CH_3): C, 23.14; H, 2.22; N, 3.86. Found: C, 24.83; H, 2.41; N, 3.47. ^{1}H NMR: 5.23 (s, 10 H); 3.28 (s, 6 H). IR (CH_2Cl_2 solution): ν_{NC} = 2160 cm^{-1}.

$(NH_4)_2MoSe_4$. In a modification of the procedure reported for $(NH_4)_2MoS_4$,[20] $(NH_4)_6Mo_7O_{24} \cdot 4H_2O$, 1.70 g (1.38 mmol) was dissolved in 100 mL of concentrated NH_4OH that had been purged with N_2. Gaseous H_2Se was introduced; the reaction was noticeably exothermic. After approximately 20 min, a deep violet crystalline product was filtered, washed with water, absolute ethanol, and anhydrous diethyl ether, and then dried in vacuo. The yield was approximately 4.0 g (93% based on starting Mo). Anal. Calcd for $H_8N_2MoSe_4$: N, 6.25; H, 1.80; Mo, 21.42; Se, 70.52. Found: N, 6.34; H, 1.72; Mo, 21.60; Se, 70.46.

$(Ph_4P)_2MoSe_4$. To an aqueous solution (25 mL) of $(NH_4)_2MoSe_4$, 0.900 g (2.01 mmol), was added a solution of 2.00 g (5.34 mmol) of Ph_4PCl in 50 mL of water. The aquamarine microcrystalline product was collected by Schlenk filtration, washed with water, absolute ethanol, and diethyl ether, and then dried in vacuo. The yield was 1.75 g (80%). The compound thus obtained may be used without further purification.

$(MeCp)_2Ru_2(PPh_3)_2MoSe_4$. This complex appears oxygen sensitive and was treated accordingly. A slurry of $(MeCp)Ru(PPh_3)_2Cl$, 0.460 g (0.611 mmol), and $(Ph_4P)_2MoSe_4$, 0.333 g (0.305 mmol), were heated in 60 mL of refluxing CH_3CN for 24 h. The olive green precipitate was collected by Schlenk filtration, washed with 50 mL of CH_3CN, and recrystallized from CH_2Cl_2/CH_3CN. The yield was 0.270 g (68%) of dark green crystals. Anal. Calcd for $C_{48}H_{44}P_2Ru_2Se_4Mo$: C, 44.46; H, 3.42; Mo, 7.40; Se, 24.36. Found: C, 43.66; H, 3.63; Mo, 7.45; Se, 24.14. ^{1}H NMR: 7.35 (m, 30 H); 5.00 (m, 4 H); 4.37 (s, 4 H); 1.66 (d, 6 H). ^{31}P NMR: 52.7 (s).

$[t\text{-}BuNH_3]_2WSe_4$. Typically, 30 mL of H_2Se-saturated CH_2Cl_2 was added to a colorless solution of 0.500 g (1.06 mmol) of $W(t\text{-}NBu)_2(t\text{-}NHBu)_2$ in 15 mL of CH_2Cl_2 to give a red solution. The solution was then treated with more H_2Se for 15 min. Over the course of 4–5 h, the reaction mixture was purged with H_2Se for a 5-min period every $^1/_2$ h. The red-brown precipitate was collected by Schlenk filtration and washed with CH_2Cl_2 and hexane. The solid was then recrystallized from CH_3CN/Et_2O to give 0.300 g (43.5%) of bright red crystalline $[t\text{-}BuNH_3]_2WSe_4$.[32] Anal. Calcd for $C_8H_{24}N_2Se_4W$: C, 14.83; H, 3.73; N, 4.32; Se, 48.74. Found: C, 14.36; H, 3.35; N, 4.20; Se, 48.57.

$(MeCp)_2Ru_2(PPh_3)_2WSe_4$. $(MeCp)Ru(PPh_3)_2Cl$, 0.302 g (0.401 mmol) and $(t\text{-}BuNH_3)_2WSe_4$, 0.30 g (0.200 mmol), were heated in 50 mL of refluxing CH_3CN for 24 h. The red precipitate was collected by Schlenk filtration of the cool reaction mixture, washed with 2 × 10 mL CH_3CN, and recrystallized from CH_2Cl_2/CH_3CN. The yield was 0.175 g (63%) of purple microcrystals. Anal. Calcd for $C_{48}H_{44}P_2Ru_2Se_4W$: C, 41.64; H, 3.20; P, 4.47; Se, 22.81. Found: C, 40.92; H, 3.32; P, 4.57; Se, 22.52. ^{1}H NMR: 7.40 (m, 30 H); 4.90 (d, 4 H); 4.30 (d, 4 H); 1.73 (s, 6 H). ^{31}P NMR: 52.4 (s).

Kinetics Studies. The reactions of **1** with various quantities of *t*-BuNC were conducted in 5-mm NMR tubes with $CDCl_3$ as the solvent. After **1** had been dissolved in the solvent and its ^{1}H NMR spectrum had been measured, neat *t*-BuNC was injected into the red solution through a septum cap by using a microliter syringe. The sample was rapidly mixed and placed into the probe of a Varian XL-200 spectrometer, which was thermostated at 23 °C. The progress of the reactions were monitored

Table V. Thermal Parameters

	U_{11}, U_{iso}	U_{22}	U_{33}	U_{23}	U_{13}	U_{12}
W	0.050 (1)	0.0390 (9)	0.0449 (10)	0.0	0.0180 (7)	0.0
Ru	0.049 (1)	0.050 (1)	0.050 (1)	0.0021 (9)	0.018 (1)	0.0057 (9)
C1A	0.17 (2)	0.09 (2)	0.16 (2)	−0.04 (2)	0.05 (2)	−0.01 (2)
C1B	0.16 (2)	0.13 (1)	0.07 (1)	0.005 (10)	0.01 (1)	−0.01 (2)
S1	0.058 (4)	0.054 (4)	0.061 (4)	0.007 (3)	0.024 (4)	−0.002 (3)
S2	0.064 (5)	0.069 (4)	0.063 (5)	−0.016 (3)	0.018 (4)	0.010 (3)
N1	0.06 (1)	0.05 (1)	0.06 (1)	0.03 (1)	0.02 (1)	0.00 (1)
C1	0.05 (2)	0.09 (2)	0.09 (2)	0.01 (2)	0.05 (2)	0.01 (1)
C2	0.09 (2)	0.06 (2)	0.07 (2)	−0.04 (1)	0.02 (2)	0.01 (1)
C3	0.11 (3)	0.04 (2)	0.13 (3)	0.00 (2)	0.03 (3)	0.06 (2)
C4	0.14 (3)	0.14 (3)	0.06 (2)	0.01 (2)	0.06 (2)	0.08 (3)
C5	0.05 (2)	0.14 (3)	0.25 (5)	0.05 (3)	0.07 (3)	0.02 (2)
C6	0.11 (3)	0.30 (6)	0.09 (3)	−0.07 (3)	0.01 (3)	0.09 (4)
C7	0.15 (4)	0.20 (4)	0.16 (4)	0.11 (4)	0.13 (4)	0.12 (3)
C8	0.18 (6)					
H	0.17 (4)[a]					

[a] Group isotropic thermal parameter refined for hydrogen atoms.

by frequent (first 5-min and then 10-min intervals) measurements (32 pulses in an acquisition time of 66 s). From integrated intensities of the C_5H_5 resonances (see Figure 3), the concentrations of each species at any time were obtained. This data was used to prepare ln [A] veresus time plots. The least-squares best line was calculated for the data, and the plots were examined by using the χ^2 test. Approximate values of k_2 were obtained by examining the best fit of calculated k_1 and varied k_2 values with respect to experimental-data-derived reaction profiles. The following experiments were conducted:

1. $[\mathbf{1}]_0 = 0.0043$ M, $[t\text{-BuNC}]_0 = 0.0172$ M; $k_1 = 0.000\,56$ s^{-1} ($\chi^2 = 1.024$).
2. $[\mathbf{1}]_0 = 0.0043$ M, $[t\text{-BuNC}]_0 = 0.0258$ M; $k_1 = 0.000\,41$ s^{-1} ($\chi^2 = 1.764$).
3. $[\mathbf{1}]_0 = 0.0054$ M, $[t\text{-BuNC}]_0 = 0.0645$ M; $k_1 = 0.000\,72$ s^{-1} ($\chi^2 = 2.161$). Experiment 3 was repeated by using an internal standard of hexamethylbenzene to confirm that mass balance was preserved throughout the reaction.

X-ray Crystallography. Single crystals of $Cp_2Ru_2(MeNC)_2WS_4 \cdot CH_2Cl_2$ were obtained by layering a CH_2Cl_2 solution of the complex with pentane. The dark red, columnar crystal used for data collection was cut from a longer crystal and was observed to extinguish plane-polarized light. The crystal was mounted in a 0.3-mm thin-walled glass capillary. The crystal decomposed rapidly in the X-ray beam, but the decay was apparently an isotropic, linear function of exposure time and a correction was applied on the basis of three standard reflections, which were monitored after every 100 intensities measured (total decay ca. 65%). Data were collected at 26 °C on a Syntex $P2_1$ automated four-circle diffractometer using graphite-monochromated molybdenum radiation. Data collection parameters are presented in Table III. The data were corrected for Lorentz and polarization effects, anomalous dispersion effects, and absorption. The alternate space group setting $I2/a$ was chosen to avoid the correlations between positional parameters anticipated for the conventional C-centered setting where $\beta = 126.23°$.

Structure Solution and Refinement. The structure was solved by Patterson methods; correct positions for the two unique metal atoms were deduced from a sharpened Patterson map. A weighted difference Fourier synthesis gave positions for the sulfur atoms and subsequent least-squares–difference Fourier calculations revealed positions for the remaining non-hydrogen atoms (including a methylene chloride solvate molecule disordered about the 2-fold axis). The hydrogen atoms of the trimer were fixed in "idealized" positions; the hydrogen atoms of the solvate molecule were not included in the structure factor calculations. In the final cycle of least-squares refinement, all non-hydrogen atoms of the trimer and the chlorine atoms of the disordered solvate molecule were refined with anisotropic thermal coefficients, atom C8 was refined with an isotropic thermal coefficient, and a group isotropic thermal coefficient parameter was varied for the hydrogen atoms. Refinement in the acentric space group Ia converged with unreasonable positions for chemically equivalent atoms in the trimer and did not improve the proposed disorder model for the solvate molecule. Successful convergence of the centric least-squares refinement was indicated by the maximum shift/error for the last cycle of 0.02. In the final difference Fourier map there was no residual electron density above the background, and the highest positive peaks were in the vicinity of the metal atoms. A final analysis of variance between observed and calculated structure factors showed no obvious systematic errors. Atomic coordinates of non-hydrogen atoms and thermal parameters are presented in Tables IV and V.

Acknowledgment. This research was funded by the National Science Foundation.

Supplementary Material Available: Tables of atomic coordinates, thermal parameters, and bond lengths and angles (3 pages); a table of final observed and calculated structure factors (3 pages). Ordering information is given on any current masthead page.

Contribution from the Department of Chemistry and Biochemistry, University of California, Los Angeles, Los Angeles, California 90024-1569

Synthesis and Structural Characterization of Copper(I) Cupracarboranes. A Novel "Pinwheel" Cluster

Han Chyul Kang, Youngkyu Do, Carolyn B. Knobler, and M. Frederick Hawthorne*

Received December 2, 1987

Synthesis and structural characteristics of copper(I) complexes of [*nido*-7,8-$C_2B_9H_{10}L]^{n-}$ (**1**, L = H, n = 2; **2**, L = 4-$(C_5H_4N)CO_2CH_3$, n = 1) are reported. Reaction systems with variable 1:CuCl:PPh_3:(PPN)Cl and **2**:CuCl:PPh_3 mole ratios have resulted in the following cupracarboranes: [*closo*-3-(PPh_3)-3,1,2-$CuC_2B_9H_{11}]^-$ (**3**), [*closo-exo*-4,8-{$(\mu$-H)$_2$Cu(PPh_3)}-3-(PPh_3)-3,1,2-$CuC_2B_9H_9$] (**4**), [*closo*-3-(PPh_3)-4-L-3,1,2-$CuC_2B_9H_{10}$] (**5**, L = 4-$(C_5H_4N)CO_2CH_3$), and [$Cu_3(\mu$-H$)_3(C_2B_9H_9L)_3$] (**6**, L = 4-$(C_5H_4N)CO_2CH_3$). These compounds have been structurally characterized by single-crystal X-ray diffraction. Crystallographic parameters are as follows (compound: crystal system; space group; crystal parameters; Z; unique data ($I > 3\sigma(I)$); R, R_w). PPN[**3**]: monoclinic; $P2_1/n$; a = 11.507 (1) Å, b = 14.772 (1) Å, c = 30.751 (2) Å, β = 90.284 (2)°; 4; 4831; 6.4, 7.6. **4**: monoclinic; $P2_1/n$; a = 10.005 (2) Å, b = 20.693 (4) Å, c = 18.998 (3) Å, β = 92.664 (6)°; 4; 5071; 4.5, 6.1. **5**: monoclinic; $P2_1/c$; a = 13.798 (1) Å, b = 12.072 (1) Å, c = 18.845 (2) Å, β = 95.111 (3)°; 4; 2290; 7.1, 8.3. **6**·n-C_7H_{16}: rhombohedral; $R\bar{3}$; a = 17.280 (4) Å, c = 28.630 (7) Å; 6; 2309; 6.5, 10.6. The polyhedral CuC_2B_9 framework is a common structural feature displayed by all four cupracarboranes. The geometry of this cage framework varies in such a way that opening of the (d^{10}-M)C_2B_9 icosahedra increases in the order **3**, **4**, **5**, and **6**, resulting in closo geometry for **3** and **4**, nido geometry for **6**, and an intermediate geometry for **5**. Two copper(I) centers in **4** are associated with one carborane cage via the open pentagonal C_2B_3 face and two B-H-Cu bridges. Both bridging BH units originate from the upper pentagonal belt of the dicarbollide moiety, resulting in an interatomic Cu(I)–Cu(I) distance of 2.576 (1) Å. In a formal sense, **4** is a zwitterion composed of an anionic **3** complexed with a $[Cu(PPh_3)]^+$ cation. The dinuclear structural integrity of **4** remains intact upon dissolution, although fluxional processes become operative, as revealed by variable-temperature multinuclei FT NMR spectroscopy. The trinuclear cupracarborane **6** contains three [$CuC_2B_9H_{10}$(4-$(C_5H_4N)CO_2CH_3$)] units, which are linked by both Cu–H–B and Cu–Cu (2.519 (2) Å) interactions about a crystallographic 3-fold axis such that a "pinwheel" ligand array around an equilateral Cu_3 core results. Compound **6** represents an example of a "clustered cluster". The extent of metal–metal interactions in **4** and **6**, as implied by their relatively short copper–copper distances, is discussed. Structural comparison of these copper(I) complexes suggests that the substituent at boron is not electronically "innocent" with respect to molecular distortions.

Introduction

Recent developments of the chemistry of the dicarbollide anion [*nido*-7,8-$C_2B_9H_{11}]^{2-}$ (**1**),[1] a unique ligand type, have proceeded with great diversity, ranging over immunological applications,[2] cluster catalysis,[3] hypervalency in nonmetals,[4] and the synthesis of clustered clusters.[5] The foregoing variety in dicarbollide

(1) (a) Hawthorne, M. F.; Young, D. C.; Andrews, T. D.; Howe, D. V.; Pilling, R. L.; Pitts, A. D.; Reintjes, M.; Warren, L. F., Jr.; Wegner, P. A. *J. Am. Chem. Soc.* **1968**, *90*, 879. (b) Alder, R. G.; Hawthorne, M. F. *J. Am. Chem. Soc.* **1970**, *92*, 6174.

(2) Mizusawa, E. A.; Thompson, M. R.; Hawthorne, M. F. *Inorg. Chem.* **1985**, *24*, 1911.

(3) Hawthorne, M. F. In *Chemistry for the Future, IUPAC*; Grunewald, H., Ed.; Pergamon: New York, 1984; p 135.

(4) Schubert, D. M.; Rees, W. S., Jr.; Knobler, C. B.; Hawthorne, M. F. *Pure. Appl. Chem.* **1987**, *59*, 869.

0020-1669/88/1327-1716$01.50/0